Published in final edited form as:
ACS Nano. 2009 December 22; 3(12): 3854. doi:10.1021/nn9010126.

Near Infrared Fluorescent NanoGUMBOS for Biomedical Imaging

David K. Bwambok[1], **Bilal El-Zahab**[1], **Santhosh K. Challa**[1], **Min Li**[1], **Lin Chandler**[2], **Gary A. Baker**[3], and **Isiah M. Warner**[*,1]

[1] Department of Chemistry, Louisiana State University, Baton Rouge, LA, 70803

[2] Horiba Jobin Yvon Inc., Edison, NJ, 08820

[3] Chemical Sciences Division, Oak Ridge National Laboratory, Oak Ridge, TN 37831

Abstract

Herein, we report on near infrared (NIR) fluorescent nanoparticles generated from an emergent class of materials we refer to as a **G**roup of **U**niform **M**aterials **B**ased on **O**rganic **S**alts (GUMBOS). GUMBOS are largely frozen ionic liquids, although the concept is more general and is also easily applied to solid ionic materials with melting points in excess of 100 °C. Nanoparticles based on GUMBOS (nanoGUMBOS) derived from a NIR fluorophore are prepared using a reprecipitation method and evaluated for *in vivo* fluorescence imaging. Due to their uniformity, single-step preparation, and composite nature, nanoGUMBOS help to resolve issues with dye leakage problems innate to alternate cellular stains and unlock a myriad of applications for these materials, highlighting exciting possibilities for multifunctional nanoGUMBOS.

Keywords

Near infrared; fluorescence; ionic liquids; GUMBOS; nanoparticles; nanoGUMBOS; biomedical imaging

Near infrared (NIR) fluorescent materials have been successfully applied in areas such as analyses and sensor development,[1] laser dyes,[2] organic light-emitting diodes (OLEDs),[3] invisible printing inks,[4] photodynamic therapy,[5] and as biomedical imaging contrast agents.[6–10] For *in vivo* imaging applications, the low absorption coefficient of human skin tissues in the 700–1100 nm NIR wavelength region[11] minimizes scattering and background interference, allowing for deep tissue imaging.[12] A number of NIR-emissive materials have been exploited based on their desirable luminescence in this spectrally quiet region, especially those that fall in the nano-regime. These nanomaterials include quantum dots,[13] single walled carbon nanotubes,[14] lanthanides,[15] fluorescent proteins,[16] gold nanoshells,[12] fluorophore-tagged polymers,[17] and organic dyes.[18,19] However, many of these nanomaterials have had concerns raised regarding both their environmental safety and their cytotoxicity. For instance, quantum dots have been reported to cause microbial toxicity[20] and pose serious environmental safety concerns which are difficult to either control or predict. In this regard, the development of alternative nanomaterials that are biocompatible, non-toxic, and tunable, while exhibiting well-defined delivery behavior, is highly sought.

*Corresponding author. iwarner@lsu.edu (Isiah M. Warner), Phone (225) 578-2829; Fax (225) 578-3971.

Supporting Information Available. The yields, melting point, aqueous solubility, NMR spectra (^{1}H, ^{19}F NMR), elemental analysis of HMT derived GUMBOS; absorbance, fluorescence and size of HMT derived nanoGUMBOS. This information is available free of charge via the Internet at http://pubs.acs.org.

When employed for biological applications such as imaging, fluorophores are typically encapsulated or doped into a polymeric[21] or silica[22] carrier particle, primarily for purposes of biocompatibility. However, dye encapsulation using these materials often leads to additional challenges such as dye leakage[21] and permeability problems.[23] There are also concerns that the use of surfactant stabilizers in the preparation of these particles may induce systemic toxicity.[24] Again, an urgent need remains for the development of uniform, non-leaking, and additive-free luminescent particles for bio-imaging.

Within our laboratories, we have recently developed an emergent class of highly promising nano-materials we will collectively refer to as GUMBOS (**G**roup of **U**niform **M**aterials **B**ased on **O**rganic **S**alts). A range of stable GUMBOS can be formed in the nano-regime from ionic liquids (ILs) that melt above physiological temperature. In general, the low melting points of ILs stem from the asymmetry of the component ions and the resultant poor crystal packing,[25] a feature open to design. Of course, nanoGUMBOS developed from ILs enjoy many of the unique properties associated with this class of material, including negligible vapor pressure, variable solubility, non-flammability, high thermal stability, ionic conductivity, and recyclability.[26] In the current application, however, GUMBOS formed from ionic materials that do not comply with the traditional working definition of an IL and melt above 100 °C[27] are also useful building blocks in GUMBOS formation. The most attractive feature of nanoGUMBOS is the ability to gather within the same nano-object several complementary or orthogonal properties, leading to the prospect of developing multifunctional GUMBOS. This designer characteristic borrows from lessons learned in IL technology, namely, that careful selection and pairing of a functional cation with a dissimilarly functional anion leads to a tailored material displaying bimodal properties.

In this study, we report on a class of fluorescent nanoparticle based on the concept of GUMBOS. These nanoparticles display uniform, stable NIR luminescence suitable for fluorescence imaging applications. As proof of concept, the unique spectral properties of [HMT][AOT] nanoGUMBOS and its performance in cellular imaging studies is summarized in this work. To the best of our knowledge, this is the first report of IL-based NIR fluorescent nanoparticles. Our results suggest that nanoGUMBOS might offer unique possibilities for *in vivo* NIR fluorescence imaging without the need for dye carriers, providing potential as contrast agents in other medical imaging modes as well.

RESULTS AND DISCUSSION

Synthesis, Characterization and Optical Properties of NIR GUMBOS and NanoGUMBOS

The GUMBOS reported in this manuscript were produced from a cationic NIR core unit following a modification of anion exchange procedures reported elsewhere.[28–30] We selected for this study, a model cationic NIR-emitting cyanine dye 1,1′,3,3,3′,3′-hexamethylindotricarbocyanine (HMT) iodide. We note that cyanine dyes such as indocyanine green (commonly known as cardiogreen) is approved by the FDA for use in bioimaging in coronary angiography, evaluation of hepatic function and monitoring blood flow.[31–34] For studies involving human cells or animal models, more careful choices of non-toxic NIR dyes is of paramount importance.

An example of an anion exchange reaction between HMT iodide and sodium bis (2-ethylhexyl) sulfosuccinate (AOT) is shown in Scheme 1. We note that AOT has been previously used as anion to make ILs.[35] The various anions used in the formulation of our GUMBOS were selected for their varying hydrophobicities, geometries, and masses. All GUMBOS obtained were characterized by nuclear magnetic resonance (NMR) and elemental microanalysis and yielded results consistent with expectations and the data is provided in the supporting information (Figure S1, Tables S1 and S2).

As expected, the resulting NIR-emitting GUMBOS displayed variable physical properties (melting point, solubility) dependent upon variations in the anion (Table S1). This illustrates the tunability of our GUMBOS, allowing the design of a variety of physicochemical properties targeting select applications. In general, we found that the melting point decreased with an increase in the size of the anion for borate containing anions. For instance, HMT with a relatively smaller tetrafluoroborate anion had a melting point of 175°C whereas the melting point decreased to 95°C when a larger 3,5 bis (trifluoromethyl) phenyltrifluoroborate anion was used (Table S1). This observation is consistent with that of Larsen and coworkers who investigated the factors that affect melting point for imidazolium ILs.[36] The authors concluded that the reduced crystal packing efficiency resulting from large anion incorporation played a profound role in depressing the melting point. Additionally, alkylation of the anion further frustrated the ion packing, causing a further drop in the melting point.[36] It is worth noting that databanks and semi-empirical models to predict melting points of ILs have been published.[37] References such as these serve as valuable resources when considering the design and synthesis of future GUMBOS.

The solubility of ILs in water has been shown to be highly dependent on the choice of the anion.[38] As expected, the miscibility of the various GUMBOS with water was also highly variable and dependent on the anion used in GUMBOS formation. The water-immiscible GUMBOS are suggestive of poor hydrogen bonding interactions, as exemplified by [HMT][AOT]. However, some GUMBOS based on relatively hydrophilic iodide and boron-containing anions such as tetrafluoroborate showed enhanced aqueous solubility, possibly a consequence of the additional hydrogen bonding afforded by the degree of fluorination. In addition, the electron-withdrawing properties of fluorine may induce dipole moments, resulting in dipole–induced dipole interactions with the surrounding water molecules.[39] This postulate is supported by water immiscibility of HMT containing the 3,5 bis (trifluoromethyl) phenyltrifluoroborate anion which may be attributed to a reduced net dipole moment arising from symmetric trifluoromethyl substitution (Table S1).

In each case, solutions of GUMBOS based on the [HMT] cation were excellent absorbers of NIR irradiation. An example of this observation is shown in Figure 1A for a 1.0 μM ethanolic solution of [HMT][AOT] GUMBOS, where peak absorption occurs at 743 nm. As a result of the parent HMT cation, the GUMBOS fluoresce strongly in the NIR region, peaking near 765 nm, with the fluorescence excitation and emission spectra following the mirror-image rule (Figure 1B) as expected from the Franck-Condon principle. The fluorescence of equimolar [HMT][I] and [Na][AOT] ethanolic mixture was identical to that of [HMT][AOT] GUMBOS ethanolic solution shown in Figure 1B. Unlike in the nanoGUMBOS, the anion does not have pronounced influence on the fluorescence emission of the cationic dye in dilute solution.

In the initial report on the preparation of nanoGUMBOS, we set forth a precedent for employing frozen ILs to manufacture size-controlled nanoparticles.[40] In our earlier study, we developed a “melt-emulsion-quench” approach for the controllable formation of particles with average diameters spanning the 45 to 3000 nm range. In the current work, the preparation of nanoGUMBOS was achieved using a modified reprecipitation method,[41–45] which is simpler to implement and more rapid. In a typical preparation, 100 μL of a 1 mM solution of GUMBOS precursor dissolved in ethanol was rapidly injected into 5 mL of triply-deionized water in an ultrasonic bath, followed by further sonication for 2 min. The ethanolic pre-GUMBOS solution and water were both filtered prior to preparation of the nanoparticles using 0.2 μm nylon membrane filters. Post-preparation, the particle suspension was aged for 1 h in the dark. The average particle size and size distribution of the prepared nanoGUMBOS were obtained by use of transmission electron microscopy (TEM) and dynamic light scattering (DLS). We note that most of the water miscible solvents such as acetonitrile, tetrahydrofuran, dimethyl

sulfoxide, N-methyl pyrrolidinone, and acetone may be used in reprecipitation to obtain nanoGUMBOS dispersed in water.

The reprecipitation synthetic method yields primarily spherical or slightly ovate nanoparticles as confirmed by TEM. A representative TEM micrograph of nanoGUMBOS with an average particle diameter of 71±16 nm is shown in Figure 2A. The polydispersity index obtained for these samples by use of DLS was generally quite good, usually under 0.100. The average size and size distribution of other nanoGUMBOS is provided in the supporting information (Table S1).

The prepared NIR-emitting nanoGUMBOS displayed optical properties which were strikingly different from that of the initial ethanolic dye solution. The absorbance and fluorescence spectra of all the nanoGUMBOS investigated are shown in the supporting information (Figure S2). The absorbance spectra for our nanoGUMBOS were generally broad and bimodal, extending to significantly lower wavelengths. For example, the absorbance of the [HMT][AOT] suspension was very broad, spanning from well below 600 nm to well over 800 nm (Figure 2B). When measured at an equivalent absorbance value, the emission intensity for the nanoparticle suspension was of comparable intensity but hypsochromically shifted by roughly 8 nm as compared to the parent compound dissolved in an EtOH solution (Figure 2C). This observation is highly characteristic of dye aggregation,[41,46] in this case reflecting intermolecular interactions between [HMT^+] units. The deconvoluted spectral properties of the nanoGUMBOS suggest that both H- and J- aggregates form in different proportions. The predominant aggregates formed seem dependent on the structure of the anion resulting in different arrangements of molecules in the nanoGUMBOS.

Decreased fluorescence intensity has also been observed for highly crystalline systems as a result of enhanced internal conversion processes.[41,46] However, we can essentially rule out this possibility as powder X-ray diffraction measurements (data not shown) of the dried nanoGUMBOS reveal that the particles are in fact predominantly amorphous (see also the SAED pattern inset in Figure 2A). Such X-ray diffraction patterns have been previously used to confirm amorphous nature of nanoparticles.[44]

If the [HMT^+]-derived nanoGUMBOS are dried and then redissolved in ethanol, they retain the spectral characteristics of the parent solution (Figure 3). This observation supports our contention that the remarkable variations in both absorbance and fluorescence properties wholly arise from the aggregation state of the [HMT^+] within the nanoGUMBOS material. This also demonstrates that the intrinsic spectroscopic properties and chemical identity of the GUMBOS precursor (‘monomer’ ion units) remain unaltered during nanoparticle formation. This observation is important when considering the potential of GUMBOS for use as drug delivery and therapeutic vehicles.

Cellular Uptake of NanoGUMBOS

In order to demonstrate the potential of nanoGUMBOS as contrast agents for biomedical imaging applications, we examined cellular uptake and fluorescence images of these particles using monkey kidney fibroblast (Vero) cells. Vero cells have previously been used for screening *E. coli* toxin and can serve as host cells for viruses as well as eukaryotic parasites. In the present study, Vero cells were used as model cells to investigate the cellular uptake of our nanoGUMBOS. Using an epifluorescence microscope, we captured fluorescence images revealing that [HMT][AOT] nanoGUMBOS can be internalized and subsequently visualized within viable Vero cells after 24 h of incubation (Figure 4). These studies suggest the exciting potential of using nanoGUMBOS in cellular imaging. The apparent homogeneous fluorescence suggests that the nanoGUMBOS distribute nonspecifically inside the cells and are primarily located within the cytoplasm. The uptake of these nanoparticles is presumably due to the well

known adsorptive endocytosis process previously demonstrated for mesoporous silica nanoparticles;[47] however, the exact cell-penetrating mechanism and localization of the nanoparticles is currently under investigation.

CONCLUSIONS

In summary, we have synthesized and investigated preliminary spectral and cellular uptake properties of a series of NIR fluorescent nanoscale ionic materials we term nanoGUMBOS. By appropriate selection of a cationic NIR dye, these fluorescent nanoparticles were designed to exhibit absorbance and luminescent properties in the tissue-accessible NIR region of the electromagnetic spectrum. In this study, nanoGUMBOS 71±16 nm in diameter were fabricated by use of a simple, rapid, repeatable, and additive-free reprecipitation method requiring neither special nor costly lab apparatus. Beyond the ease of preparation, this work presents an entirely non-conventional direction for preparing contrast agent nanoparticles directly from tailored ionic materials. Our approach alleviates current problems associated with dye leakage and other challenges encountered in dye encapsulation, as well obviating intensive purification steps required when surfactants are used to prepare dye nanoparticles. It is also noteworthy that the spectral properties of our GUMBOS deviate markedly from the freely dissolved dye present in solution. Thus, the possibility for tuning the optical properties of GUMBOS by variation in the parent ions offers a unique and exciting advantage for these nanomaterials. It was also demonstrated that these NIR fluorescent nanoparticles could be efficiently taken up *in vitro* by Vero cells, suggesting intriguing potential for non-invasive biomedical imaging. Even more exciting is the prospect of tailoring nanoGUMBOS for delivery into designated cellular structures. In any case, examination of the data presented for these cellular studies highlights a new potential for biomedical imaging using NIR fluorescent nanoGUMBOS.

It should be possible to extend the findings from this investigation to fashion GUMBOS combining diverse functionalities (e.g., redox, superparamagnetic, luminescent, thermochromic, ligating) in order to arrive at truly multifunctional hybrid materials. One could easily envision future polyfunctional nanoGUMBOS with applications including targeted diagnosis and therapy, photothermal cancer therapy, scintillators, radiosensitizers, biological separations, solar cells, and materials with defense applications (e.g., microwave-absorbers, security barcodes). The incorporation of high atomic number elements such as iodine or gold may enable their use as contrast agents for X-ray computed tomography (CT) scans. Likewise, GUMBOS carrying gadolinium chelates may open up potential for clinical diagnosis by use of magnetic resonance imaging (MRI).

MATERIALS AND METHODS

Materials

1,1′,3,3,3′,3′-hexamethylindotricarbocyanine (HMT) iodide (97%), bis(2-ethylhexyl) sulfosuccinate (AOT) sodium salt (≥99%), sodium tetrafluoroborate (≥98%) and potassium 3,5-bis(trifluoromethyl)phenyltrifluoroborate, lithium bis(trifluoromethane)sulfonimide (99.95%) and ethanol (spectroscopic grade) were purchased from Sigma Aldrich and used as received. Triply deionized water (18.2 MΩ cm) from an Elga model PURELAB ultra™ water filtration system was used for all preparations of the NIR GUMBOS and nanoGUMBOS. A BRANSON 3510R-DTH model bath ultrasonicator (335 watts, 40 kHz frequency) at room temperature was used in the preparation of nanoGUMBOS. Vero cells were obtained from the School of Veterinary Medicine (Louisiana State University, Baton Rouge, LA). Carbon coated copper grids (CF400-Cu, Electron Microscopy Sciences, Hatfield, PA) were used for TEM imaging.

Synthesis and characterization of NIR GUMBOS

The NIR GUMBOS (mostly ILs) were prepared using anion exchange procedures similar to those reported in the literature.[25–27] The synthesis of 1,1′,3,3,3′,3′-hexamethylindotricarbocyanine bis(2-ethylhexyl) sulfosuccinate ([HMT] [AOT]) is described as a representative procedure. An amount of 30 mg (0.056 mmol) of 1,1′,3,3,3′,3′-hexamethylindotricarbocyanine (HMT) iodide and 24.86 mg (0.056 mmol) of sodium bis (2-ethylhexyl) sulfosuccinate (AOT) salt were dissolved in a mixture of methylene chloride and water (2:1 v/v) and allowed to stir for 12 hrs at room temperature (Scheme 1). The methylene chloride bottom layer was washed several times with water and the product was obtained from the organic lower layer and dried by removal of solvent *in vacuo*. Further freeze drying to remove traces of water afforded 43.02 mg (93% yield) of [HMT] [AOT]. All GUMBOS obtained were characterized by ^{1}H NMR (Bruker Avance 400, $CDCl_3$) and elemental microanalysis (Atlantic Microlab, Norcross, GA, USA). In addition, ^{19}F NMR (Bruker DPX 250, $CDCl_3$) was used to confirm anion exchange for fluorine containing anions. Melting points of the GUMBOS was determined using a MEL-TEMP® capillary melting point apparatus.

Synthesis of NIR nanoGUMBOS

The nanoGUMBOS were prepared from GUMBOS using a modified simple, additive-free reprecipitation method similar to that used for organic nanoparticles.[24,28–31] In a typical preparation, 100 μL of a 1 mM solution of GUMBOS precursor dissolved in ethanol was rapidly injected into 5 mL of triply-deionized water in an ultrasonic bath, followed by further sonication for 2 min. The ethanol and water were both filtered prior to preparation of the nanoGUMBOS using 0.2 μm nylon membrane filters. Post-preparation, the particle suspension was aged for 1 h in the dark.

Characterization of size and morphology of NIR nanoGUMBOS

The average particle size and size distribution of the prepared nanoGUMBOS were obtained by use of transmission electron microscopy (TEM) and dynamic light scattering (DLS). TEM micrographs were obtained using an LVEM5 transmission electron microscope (Delong America, Montreal, Canada). The NIR nanoGUMBOS dispersion (1 μL) was dropcasted onto a carbon coated copper grid and allowed to dry in air at room temperature before TEM imaging.

X-ray diffraction analysis of NIR nanoGUMBOS

X-ray diffraction measurements of dried nanoGUMBOS were obtained on a Nonius Kappa CCD diffractometer by long exposures with Mo Kα radiation and rotation of samples about the vertical axis.

Absorption and fluorescence studies of NIR GUMBOS and nanoGUMBOS

Absorbance measurements were performed on a Shimadzu UV- 3101PC UV-Vis-near-IR scanning spectrometer (Shimadzu, Columbia, MD). Fluorescence emission was collected using a Spex Fluorolog-3 spectrofluorimeter (model FL3-22TAU3); Jobin Yvon, Edison, NJ). A 0.4 cm^2 quartz cuvette (Starna Cells) was used to collect the fluorescence and absorbance against an identical cell filled with water as the blank.

Cellular uptake studies of Nano-GUMBOS by Vero cells

Vero cells (isolated from kidney epithelial cell lining extracted from an African green monkey, *Cercopithecus aethiops*) were used as a model cell line for this study using HMT AOT nanoGUMBOS. The cells were maintained in Dulbecco's Modified Eagle's Medium (DMEM) before studies. The Vero cells are then loaded into an eight well glass plate (2.5×10^5 cells/well) and incubated with HMT AOT nanoparticles (8 μg/mL) for 24 hrs. The cells are then

washed twice with phosphate buffered saline (PBS) and immediately visualized using a Zeiss epifluorescence microscope equipped with a Zeiss digital camera for image acquisition. Negative controls were also prepared by loading the Vero cells into the wells which did not contain dye.

Supplementary Material

Refer to Web version on PubMed Central for supplementary material.

Acknowledgments

I.M. Warner acknowledges the National Institutes of Health (NIH) (grant number 1R01GM079670), the National Science Foundation (NSF) (grant number CHE-0616824), and the Phillip W. West Endowment for support of this work. We thank Dr. Gus Kousolas and Dmitry Chouljenko for assistance with cellular imaging. The authors are also grateful to Professor Franck Fronczek for X-ray diffraction analysis. We also thank Mr. Aaron Tesfai for technical assistance.

References

1. Barone PW, Parker RS, Strano MS. In Vivo Fluorescence Detection of Glucose Using a Single-Walled Carbon Nanotube Optical Sensor: Design, Fluorophore Properties, Advantages, and Disadvantages. Anal Chem 2005;77:7556–7562. [PubMed: 16316162]
2. Shealy DB, Lohrmann R, Ruth JR, Narayanan N, Sutter SL, Casay GA, Evans L III, Patonay G. Spectral Characterization and Evaluation of Modified near-Infrared Laser Dyes for DNA Sequencing. Appl Spectrosc 1995;49:1815–20.
3. Qian G, Zhong Z, Luo M, Yu D, Zhang Z, Ma D, Wang ZY. Synthesis and Application of Thiadiazoloquinoxaline-Containing Chromophores as Dopants for Efficient near-Infrared Organic Light-Emitting Diodes. J Phys Chem C 2009;113:1589–1595.
4. Yousaf M, Lazzouni M. Formulation of an Invisible Infrared Printing Ink. Dyes Pigm 1995;27:297–303.
5. Zhang P, Steelant W, Kumar M, Scholfield M. Versatile Photosensitizers for Photodynamic Therapy at Infrared Excitation. J Am Chem Soc 2007;129:4526–4527. [PubMed: 17385866]
6. Umezawa K, Citterio D, Suzuki K. A Squaraine-Based near-Infrared Dye with Bright Fluorescence and Solvatochromic Property. Chem Lett 2007;36:1424–1425.
7. Fabian J, Nakazumi H, Matsuoka M. Near-Infrared Absorbing Dyes. Chem Rev 1992;92:1197–1226.
8. Law KY. Organic Photoconductive Materials: Recent Trends and Developments. Chem Rev 1993;93:449–86.
9. Jobsis FF. Noninvasive, Infrared Monitoring of Cerebral and Myocardial Oxygen Sufficiency and Circulatory Parameters. Science 1977;198:1264–7. [PubMed: 929199]
10. Kim S, Lim YT, Soltesz EG, De Grand AM, Lee J, Nakayama A, Parker JA, Mihaljevic T, Laurence RG, Dor DM, et al. Near-Infrared Fluorescent Type Ii Quantum Dots for Sentinel Lymph Node Mapping. Nat Biotechnol 2004;22:93–97. [PubMed: 14661026]
11. Bashkatov AN, Genina EA, Kochubey VI, Tuchin VV. Optical Properties of Human Skin, Subcutaneous and Mucous Tissues in the Wavelength Range from 400 to 2000 Nm. J Phys D: Appl Phys 2005;38:2543–2555.
12. Loo C, Lowery A, Halas N, West J, Drezek R. Immunotargeted Nanoshells for Integrated Cancer Imaging and Therapy. Nano Lett 2005;5:709–711. [PubMed: 15826113]
13. Bruchez M Jr, Moronne M, Gin P, Weiss S, Alivisatos AP. Science 1998;281:2013–2016. [PubMed: 9748157]
14. Welsher K, Liu Z, Daranciang D, Dai H. Selective Probing and Imaging of Cells with Single Walled Carbon Nanotubes as near-Infrared Fluorescent Molecules. Nano Lett 2008;8:586–590. [PubMed: 18197719]
15. Moore EG, Szigethy G, Xu J, Palsson LO, Beeby A, Raymond KN. 3-Hydroxypyridin-2-One Complexes of near-Infrared (Nir) Emitting Lanthanides: Sensitization of Holmium (Iii) and Praseodymium (Iii) in Aqueous Solution. Angew Chem, Int Ed 2008;47:9500–9503.

16. Shi X, Royant A, Lin MZ, Agilera TA, Lev-Ram V, Steinbach PA, Tsien RY. Mammalian Expression of Infrared Fluorescent Proteins Engineered from a Bacterial Phytochrome. Science 2009;324:804–807. [PubMed: 19423828]

17. Kim K, Lee M, Park H, Kim JH, Kim S, Chung H, Choi K, Kim IS, Seong BL, Kwon IC. Cell-Permeable and Biocompatible Polymeric Nanoparticles for Apoptosis Imaging. J Am Chem Soc 2006;128:3490–3491. [PubMed: 16536501]

18. Bringley JF, Penner TL, Wang R, Harder JF, Harrison WJ, Buonemani L. Silica Nanoparticles Encapsulating near-Infrared Emissive Cyanine Dyes. J Colloid Interface Sci 2008;320:132–139. [PubMed: 18191871]

19. Yang Y, Lowry M, Xu X, Escobedo JO, Sibrian-Vazquez M, Wong L, Schowalter CM, Jensen TJ, Fronczek FR, Warner IM, et al. Seminaphthofluorones Are a Family of Water-Soluble, Low Molecular Weight, Nir-Emitting Fluorophores. Proc Natl Acad Sci 2008;105:8829–8834. [PubMed: 18579790]

20. Derfus AM, Chan WCW, Bhatia SN. Probing the Cytotoxicity of Semiconductor Quantum Dots. Nano Lett 2004;4:11–18.

21. Saxena V, Sadoqi M, Shao J. Enhanced Photo-Stability, Thermal-Stability and Aqueous-Stability of Indocyanine Green in Polymeric Nanoparticulate Systems. J Photochem Photobiol, B 2004;74:29–38. [PubMed: 15043844]

22. Burns A, Sengupta P, Zedayko T, Baird B, Wiesner U. Core/Shell Fluorescent Silica Nanoparticles for Chemical Sensing: Towards Single-Particle Laboratories. Small 2006;2:723–726. [PubMed: 17193111]

23. Yu J, Yaseen MA, Anvari B, Wong MS. Synthesis of near-Infrared-Absorbing Nanoparticle-Assembled Capsules. Chem Mater 2007;19:1277–1284.

24. Baba K, Pudavar HE, Roy I, Ohulchanskyy TY, Chen Y, Pandey RK, Prasad PN. New Method for Delivering a Hydrophobic Drug for Photodynamic Therapy Using Pure Nanocrystal Form of the Drug. Mol Pharmaceut 2007;4:289–297.

25. Del Popolo MG, Voth GA. On the Structure and Dynamics of Ionic Liquids. J Phys Chem B 2004;108:1744–1752.

26. Welton T. Room-Temperature Ionic Liquids. Solvents for Synthesis and Catalysis. Chem Rev 1999;99:2071–2083. [PubMed: 11849019]

27. Seddon KR, Stark A, Torres MJ. Influence of Chloride, Water, and Organic Solvents on the Physical Properties of Ionic Liquids. Pure Appl Chem 2000;72:2275–2287.

28. Del Sesto RE, McCleskey TM, Burrell AK, Baker GA, Thompson JD, Scott BL, Wilkes JS, Williams P. Structure and Magnetic Behavior of Transition Metal Based Ionic Liquids. Chem Commun 2008:447–449.

29. Bwambok David K, Marwani Hadi M, Fernand Vivian E, Fakayode Sayo O, Lowry M, Negulescu I, Strongin Robert M, Warner Isiah M. Synthesis and Characterization of Novel Chiral Ionic Liquids and Investigation of Their Enantiomeric Recognition Properties. Chirality 2008;20:151–8. [PubMed: 18092298]

30. Earle MJ, Gordon CM, Plechkova NV, Seddon KR, Welton T. Decolorization of Ionic Liquids for Spectroscopy. Anal Chem 2007;79:758–764. [PubMed: 17222047]

31. Weissleder R, Ntziachristos V. Shedding Light onto Live Molecular Targets. Nat Med 2003;9:123–8. [PubMed: 12514725]

32. Tanaka E, Chen FY, Flaumenhaft R, Graham GJ, Laurence RG, Frangioni JV. Real-Time Assessment of Cardiac Perfusion, Coronary Angiography, and Acute Intravascular Thrombi Using Dual-Channel near-Infrared Fluorescence Imaging. J Thorac Cardiov Sur 2009;138:133–140.

33. Ishihara H, Okawa H, Iwakawa T, Umegaki N, Tsubo T, Matsuki A. Does Indocyanine Green Accurately Measure Plasma Volume Early after Cardiac Surgery? Anesth Analg 2002;94:781–786. [PubMed: 11916773]

34. Caesar J, Shaldon S, Chiandussi L, Guevara L, Sherlock S. The Use of Indocyanine Green in the Measurement of Hepatic Blood Flow and as a Test of Hepatic Function. Clin Sci 1961;21:43–57. [PubMed: 13689739]

35. Hough WL, Smiglak M, Rodriguez H, Swatloski RP, Spear SK, Daly DT, Pernak J, Grisel JE, Carliss RD, Soutullo MD, et al. The Third Evolution of Ionic Liquids: Active Pharmaceutical Ingredients. New J Chem 2007;31:1429–1436.
36. Larsen AS, Holbrey JD, Tham FS, Reed CA. Designing Ionic Liquids: Imidazolium Melts with Inert Carborane Anions. J Am Chem Soc 2000;122:7264–7272.
37. Huo Y, Xia S, Zhang Y, Ma P. Group Contribution Method for Predicting Melting Points of Imidazolium and Benzimidazolium Ionic Liquids. Ind Eng Chem Res 2009;48:2212–2217.
38. Freire MG, Carvalho PJ, Gardas RL, Santos LMNBF, Marrucho IM, Coutinho JAP. Solubility of Water in Tetradecyltrihexylphosphonium-Based Ionic Liquids. J Chem Eng Data 2008;53:2378–2382.
39. van den Broeke J, Stam M, Lutz M, Kooijman H, Spek AL, Deelman B-J, van Koten G. Designing Ionic Liquids: 1-Butyl-3-Methylimidazolium Cations with Substituted Tetraphenylborate Counterions. Eur J Inorg Chem 2003:2798–2811.
40. Tesfai A, El-Zahab B, Bwambok DK, Baker GA, Fakayode SO, Lowry M, Warner IM. Controllable Formation of Ionic Liquid Micro- and Nanoparticles Via a Melt-Emulsion-Quench Approach. Nano Lett 2008;8:897–901. [PubMed: 18237150]
41. An BK, Kwon SK, Jung SD, Park SY. Enhanced Emission and Its Switching in Fluorescent Organic Nanoparticles. J Am Chem Soc 2002;124:14410–14415. [PubMed: 12452716]
42. Peng AD, Xiao DB, Ma Y, Yang WS, Yao JN. Tunable Emission from Doped 1,3,5-Triphenyl-2-Pyrazoline Organic Nanoparticles. Adv Mater 2005;17:2070–2073.
43. Gesquiere AJ, Uwada T, Asahi T, Masuhara H, Barbara PF. Single Molecule Spectroscopy of Organic Dye Nanoparticles. Nano Lett 2005;5:1321–1325. [PubMed: 16178231]
44. Xiao D, Xi L, Yang W, Fu H, Shuai Z, Fang Y, Yao J. Size-Tunable Emission from 1,3-Diphenyl-5-(2-Anthryl)-2-Pyrazoline Nanoparticles. J Am Chem Soc 2003;125:6740–6745. [PubMed: 12769584]
45. Wang F, Han MY, Mya KY, Wang Y, Lai YH. Aggregation-Driven Growth of Size-Tunable Organic Nanoparticles Using Electronically Altered Conjugated Polymers. J Am Chem Soc 2005;127:10350–10355. [PubMed: 16028947]
46. Gruszecki WI. Structural Characterization of the Aggregated Forms of Violaxanthin. J Biol Phys 1991;18:99–109.
47. Slowing I, Trewyn BG, Lin VSY. Effect of Surface Functionalization of Mcm-41-Type Mesoporous Silica Nanoparticles on the Endocytosis by Human Cancer Cells. J Am Chem Soc 2006;128:14792–14793. [PubMed: 17105274]

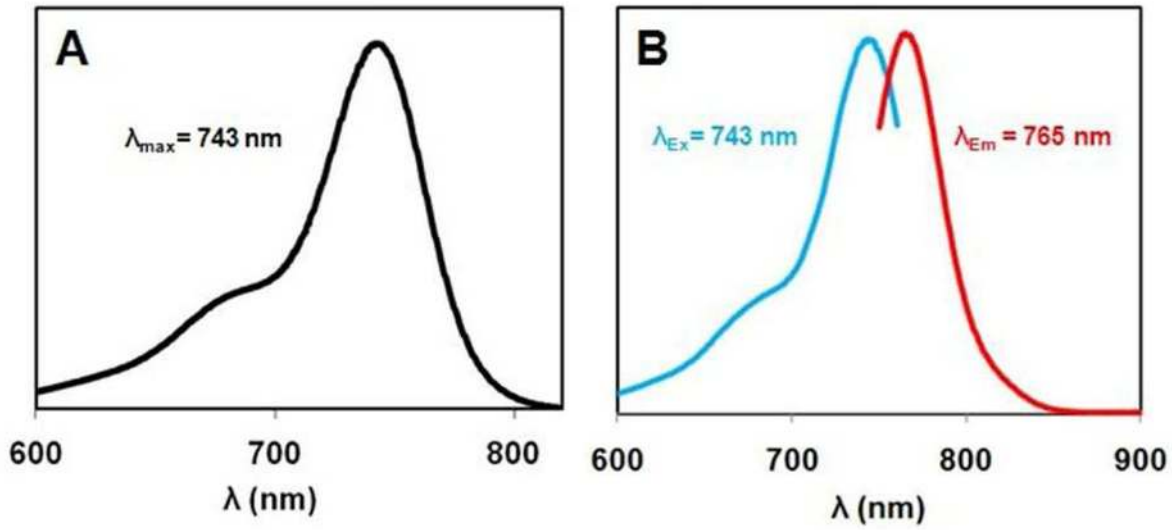

Figure 1.
(A) Absorbance profile and (B) fluorescence excitation and emission spectra for 1.0 μM [HMT] [AOT] in ethanol; λ_{ex} = 743 nm, λ_{em} = 765 nm.

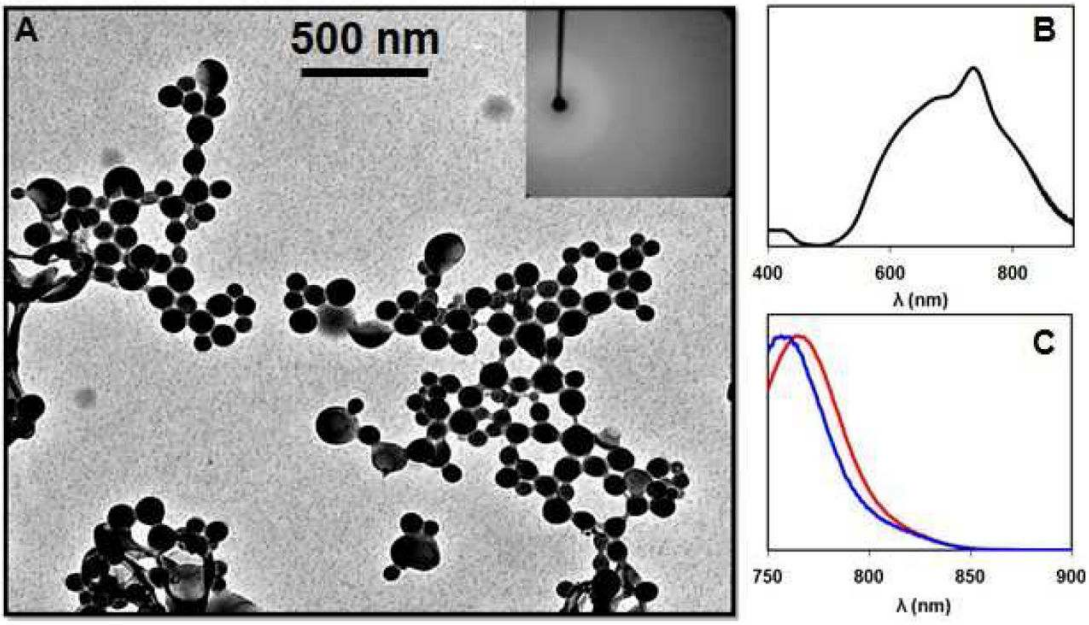

Figure 2.

(A) TEM micrograph of aqueous [HMT][AOT] fluorescent NIR nanoGUMBOS with an average diameter near 71±16 nm; the inset shows a selected area electron diffraction pattern (SAED) for the [HMT][AOT] GUMBOS. (B) Absorbance spectrum of the [HMT][AOT] nanoparticles illustrated in panel A, and (C) comparison between the normalized fluorescence emission spectrum of the freely dissolved [HMT][AOT] IL (1.0 μM in ethanol; red profile) and [HMT][AOT] nanoGUMBOS (blue profile) for matched absorptivity at the excitation wavelength (λ_{ex} = 743 nm).

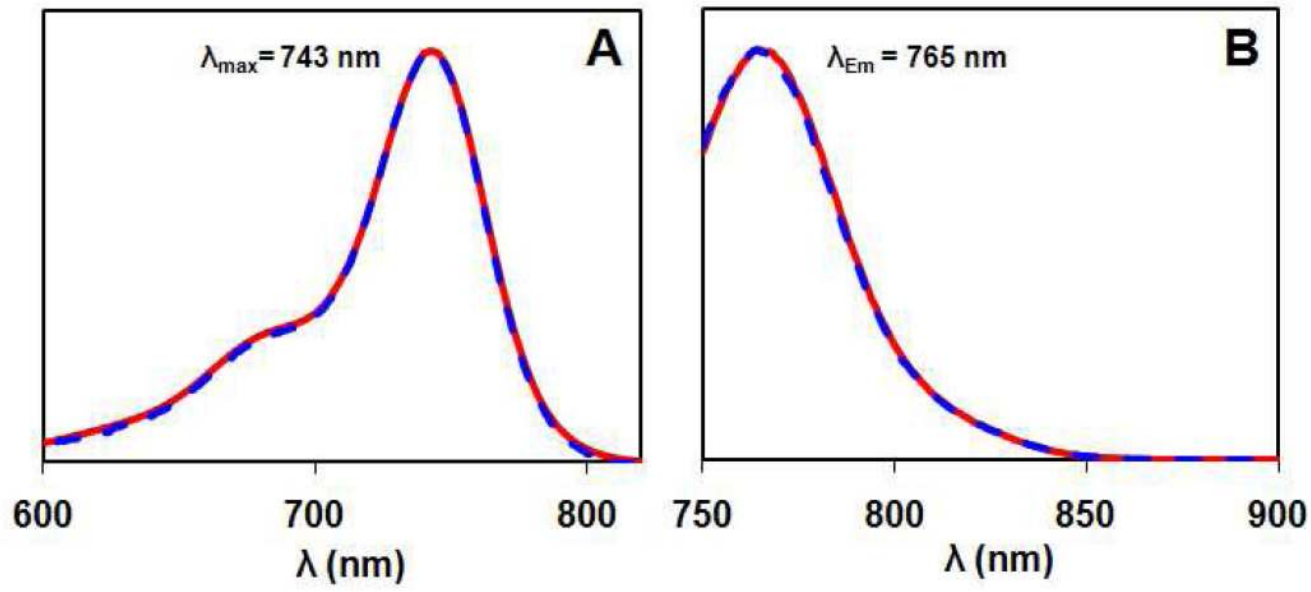

Figure 3.
Normalized (A) absorbance and (B) fluorescence emission spectra of [HMT][AOT] (1.0 μM solution in EtOH; solid curve), and GUMBOS from Figure 2A redissolved in EtOH (dashed curve).

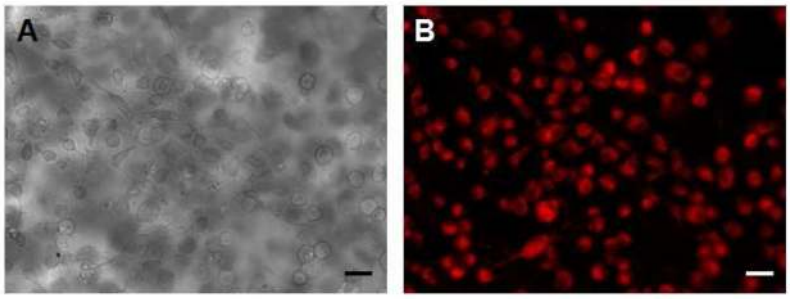

Figure 4.
Cellular uptake studies using a monkey kidney fibroblast (Vero) cell line. (A) A phase contrast micrograph and (B) the corresponding fluorescence image of Vero cells incubated for 24 h with 8.0 μg mL^{-1} [HMT][AOT] nanoGUMBOS. The fluorescence was collected using a propidium iodide (PI) filter set: λ_{ex} = 540 nm; λ_{em} = 617 nm long pass. Scale bars in (A) and (B) are 10 μm.

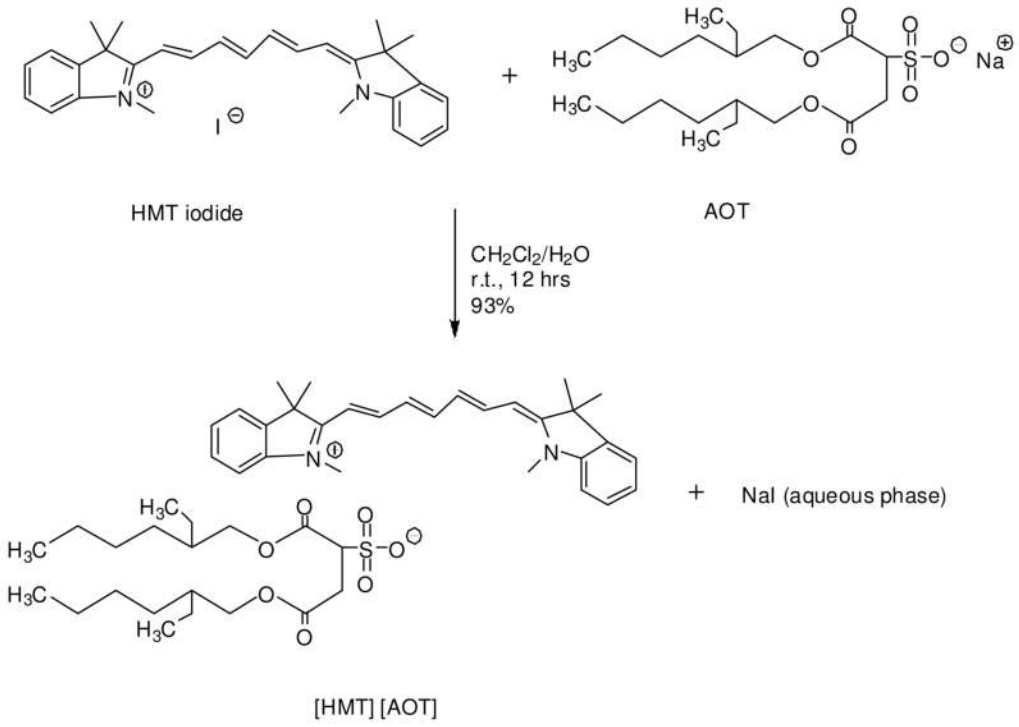

Scheme 1.
Synthesis of [HMT][AOT] by anion exchange reaction